

Blast Loading Performance of FRP Retrofitting of Two Storey Building

Namata Saidou Sabiou & Ali Koçak
Department of Civil Engineering,
Yildiz Technical University,
Istanbul, Turkey

Abstract— The use of Fiber Reinforced Polymer (FRP) is among of the advanced and efficient technologies for structural reinforcement of concrete elements in buildings. In this article the performance of FRP laminate on the lateral facade to strengthening the blast effect on the two storey building is studied.

Concept and theory of nonlinear finite element software ABAQUS is used. Explosion had taken place at two different scale distances: $Z = 0.32 \text{ [m/ (kg}^{1/3})]$ and $Z = 0.64 \text{ [m/ (kg}^{1/3})]$. Blast load is simulated by ConWep blast loading model and results are used to comparison and evaluation the retrofitted structures performance against blast loads.

Keywords— FRP; blast; finite element; building

I. INTRODUCTION

Many researches and experiments have been done to facilitate the understanding of the behavior of structural components against blast loading. Despite all this, the response of non-military structures components under explosion is relatively new area of research in comparison of the response of other forms of dynamic loading (e.g. wind and seismic); which in many cases the experimental data are relatively insufficient. So in this sense, the recent North American blast resistant design standards (ASCE) (2011) and Canadian standards association (CSA) (2012) have been focused on developing detailing techniques for civilian structures designed to withstand different combinations of blast load levels generated by a range of explosive charges and standoff distances.

The fact that existing structures are not designed to resist explosion effect, recently reported research studies have mainly focused on evaluating and improving the performance of existing reinforced concrete (RC) and steel components under blast loading Wang et al.(2012), Li et al.(2012), Nassr et al.(2012) and Stoddart et al.(2014). Other recent studies have focused on hardening (retrofit for blast) concrete components using fiber-reinforced polymer (FRP).

Rodriguez-Nikl et al. (2012) and Coughlin et al. (2010). There are many factors that have made the use of FRP composite materials of external adhesion increase as cost-effective and convenient materials for rehabilitation in case of: deterioration caused by environmental effects, impact damage, increasing of load demand due to more severe codes, especially in the seismic field, changes in the use of structures, and greater resistance and ductility to correct design or construction errors.

II. EXPLOSION PHENOMENA

An explosion is defined as a very sudden energy release in the form of light, heat, sound and shock waves, in which one part of the energy is released as thermal radiation (flash) and the other part is coupled into the air as air blast and into the soil (ground) as ground shock, both as radials expanding shock waves. The rapid expansion of hot gases resulting from the detonation of an explosive charge gives rise to compression wave called shock wave, which propagates through the air. There is nearly instantaneous rise to the peak pressure, P_{so} , and the rising time is under a microsecond. Behind the shock front, the pressure collapses and ends up being lower than the ambient temperature, later returning to ambient, P_o . The area of positive pressure is called the “positive phase” and the area of negative pressure is called “negative phase”. Overexpansion at the center of the explosion creates a vacuum in the source region and results in a reversal of motion, Kinney and Graham (1985) and causes the formation of the negative phase that trails the positive phase, T. Ngo et al. (2007). In general, the negative phase pressure is lower in magnitude than the positive phase but longer in duration than the positive phase. The blast wave instantaneously increases to a higher value of pressure than the ambient atmospheric pressure. This is referred to as the positive phase that decays as the shock wave expands outward the explosion source. After a short time, the pressure behind the front may drop under the ambient pressure (Fig.1). Positive phase loads are more powerful and responsible for most of the pressure damages than the negative phase loads. During such negative phase, partial vacuum is created and air is sucked in, which is also accompanied by high suction winds that carry the debris to long distances away from the explosion source.

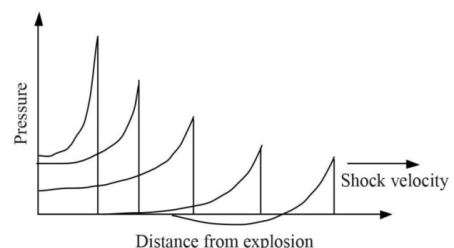


Figure 1. Blast wave propagation, T.Ngo (2007)

As the shock wave travels outside of the load, the pressure in the front of the wave, called the peak pressure, steadily decreases. At great distances from the load, the peak pressure is infinitesimal and the wave can be treated as sound wave.

III. BLAST WAVE PRESSURE TIME HISTORY

The characteristics of air blast waves are affected by the physical properties of the explosion source. Fig. 2 shows a typical blast pressure time history. At the arrival time t_A , following the explosion, pressure at that position suddenly increases to a peak value of overpressure, P_{so} , over the ambient pressure, P_o . After, the pressure decays to ambient pressure at time t_d , further to under pressure P_{so}^- (creating partial vacuum) before eventually returning to ambient conditions at time $t_d + t_d^-$. The P_{so} is usually referred to as the peak side-on overpressure, incident peak overpressure or merely peak overpressure.

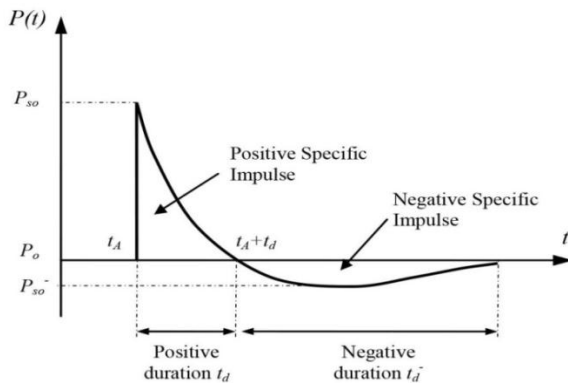


Figure 2. The time history of real blast wave in a specified position, T.Ngo (2007)

IV. SCALING FACTOR OF BLAST LOAD

Blast parameters depend mainly on the amount of energy released by the detonation in the form of an explosive wave and the distance of the explosion. A universal normalized description of the blast effects can be given by scaling distance relative to $(E/P_o)^{1/3}$ and scaling pressure relative to P_o , where E is the energy release (kJ) and P_o the ambient pressure (10197kg/m²). The principle of the scaling law is used extensively to determine blast-wave characteristics in most design guidance such as TM5-1300(1990). It is based on the conservation of momentum and geometric similarity. The empirical relationship, formulated independently by Hopkinson (1915) and Cranz (1926), is described as cube-root scaling law and is defined as:

$$Z = R/W^{1/3} \quad (1)$$

Where,

Z is the scaled distance, with units (m/kg^{1/3})

R is the range from the center of the charge

W is the mass of spherical TNT charge (kg).

V. SIMULATING AN EXPLOSION EFFECT ON THE AIR

To model the explosion effect, conventional weapon known as ConWep model which is based on experimental results obtained by Mourizt et al. (1994) and ABAQUS/Explicit (2000) software have been used. The Conwep model which assumed to be an open air explosion uses TNT equations, so, in this work, the weight of explosive is replaced by the equivalent TNT weight. In this method, the standoff distance and weight of the explosive are determined then the history of blast wave is calculated which and applied to the surface blast. The main

advantage of ConWep model is that it provides more realistic situation with considering the more detail specification of blast wave including positive and negative phases. So, there is no need to model the fluid (air) to considering the reflection effects.

According to ConWep model, the pressure exerted on a surface caused by the blast wave is a function of incident pressure $P_{incident}(t)$, reflected pressure $P_{reflect}$ and Angle of incidence θ . Pressure is defined by Mourizt as:

$$\begin{cases} P(t) = P_{incident}(t)[1 + \cos \theta - 2 \cos^2 \theta] + P_{reflect}(t) \cos^2 \theta, \cos \theta > 0 \\ P(t) = P_{incident}(t), \cos \theta < 0 \end{cases} \quad (2)$$

VI. DESCRIPTION OF THE MODEL

A building with 5 m of length, both in longitudinal and transversal direction has been used for this study. The height of each floor is 3m and the total height of the structure is 10m. The view plan of the structure is shown in Fig. 3. The structural system of the building consists of reinforced concrete frames and infill walls. The dimension of the typical beam is 400x400 mm and the column is 400 x 400 mm. For the reinforcement of the concrete, both beam and column a 2 ϕ 14 rebar is used. The distances between columns in two directions (X direction and Y direction) is 5 m and connected to the beams to support the facade. The infill wall thickness is 250 mm. The ϕ 8 is used for the reinforcement of the floor and its thickness is 150 mm.

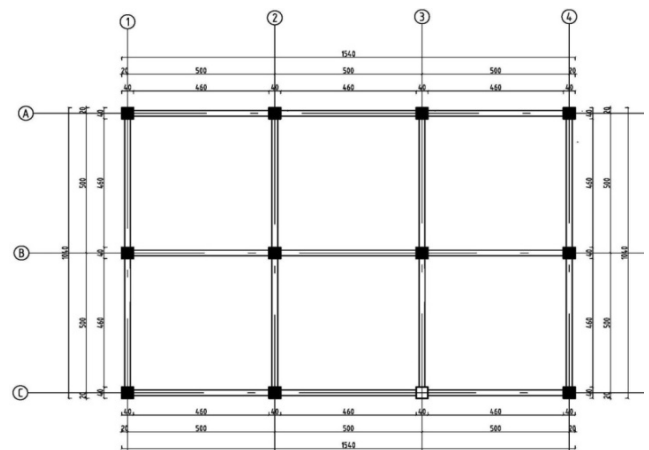


Figure 3. View plan of the structure

VII. STRUCTURAL MODELING

For numerical modelling, nonlinear 3D Finite Element Method (FEM) is utilized and the model is shown in the Fig. 4. Geometry model consisted in masonry, reinforced concrete and fiber reinforced polymer material. The masonry, which is composed with mortar and concrete blocks elements, is modelled as a homogeneous material. The whole model is meshed by 3D solid eight node element (C3D8R). The FRP material is meshed by S4R, the A 4-node doubly curved thin or thick shell, which contribute to reduce the integration. For modelling the connections between solid elements of the structure the surface- based tie connection using master-slave formulation have been used. Finally the connection between the FRP and solid element surface-based shell-to-solid coupling has been used.

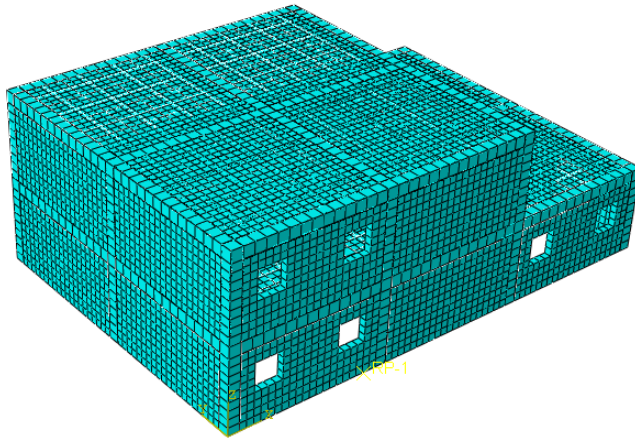


Figure. 4 Finite element model of the structure.

VIII. MATERIALS

A. Masonry and concrete

To model the concrete and masonry, Brittle Cracking Model has been used. The model assumes that the compressive behavior of concrete is always linear elastic and it is most accurate in applications where the brittle behavior dominates such that the assumption that the material is always linear elastic in compression is adequate. On the other hand the Brittle Cracking Model allows the removal of elements based on a brittle failure criterion (ABAQUS command: *BRITTLE FAILURE) avoiding in theory large distortions of elements. Parameters of the model used in this study are shown in Table.1.

TABLE I. TABLE 1 PARAMETERS OF THE BRITTLE CRACKING MODEL.

Stress	Strain	Shear		Crack		Brittle failure
3150000	0	1	0	0	0.001298183	6.49E+01
2.081.789.971	0.000288922					
1.705.996.394	0.000548379					
1.494.560.766	0.000800842					
1.353.338.316	0.001050318					
1.249.964.252	0.001298183					

B. Rebar

Density of Steel = 7850 Kg/m³; Young's modulus of Steel = 2.1×10^{11} N/m²; Poisson's ratio of Steel = 0.3. Steel plastic model parameters are showing in the Table.2.

TABLE II. TABLE 2. PLASTIC PARAMETERS OF STEEL.

Yield Stress	Plastic Strain
240754285.7	0
261512062.5	0.004553484
282960789.6	0.0091713
305870280.5	0.017922092
331191532.1	0.032798756
360055984.8	0.055599363
393775650.7	0.087802179
433843429	0.130446533
481933467.5	0.184046602
509559655.6	0.214963298
524375122.6	0.231431766

C. TNT

The charge mass was 1m above the ground. It is customary to refer the weight of explosives used in experimental tests to an equivalent weight of TNT. According to TNT equivalence calculator of the Institute of Makes Explosives (IME) [25], the different values of TNT equivalent weights were calculated and results are shown in the table 3.

TABLE III. PARAMETERS OF EXPLOSIVE MATERIAL

Charge mass, W (kg)	TNT Equivalent Weight, W _{TNT} (kg)	Stand-off distance, R (m)	Scaled distance Z=R/W ^{1/3} [m/(kg ^{1/3})]
37.00	30.00	1.0	0.32
		2.0	0.64

D. FRP

In many cases FRP and polymer materials have been used to retrofit building components against blast loads, which usually are composed of unidirectional fibers. Thus, assuming isotropic case is far from reality. In other terms, the mechanical properties of FRPs such as composites are different in various directions. Must of the time the fibers as a multilayer with epoxy resin glued to the structural member orthogonally, that's means in two perpendicular directions, mechanical properties will be different. In this paper brittle fracture model is used to simulate the behavior of FRP lamina, in which the behavior is assumed to be linear up to reach the ultimate strain (ϵ_u). In this study FRP sheets properties are intended as lamina materials, which are presented in table 2.

TABLE IV. MECHANICAL PROPERTIES OF FRP MATERIALS.

Density (kg/m ³)	E1 (GPa)	E2 (GPa)	Nu12	G12	G13	G23
1000	150	150	0.1	0.1	0.1	0.1
Ten StressFiber Dir (GPa)	Comp Stress Fiber Dir (Pa)	Ten Stress Transv Dir (GPa)	Comp Stress Transv Dir (MPa)	Shear Strength (MPa)	Cross-Prod Term Coeff	Stress Limit (GPa)
3	0.1	3	0.1	0.1	0	3

IX. RESULTS AND DISCUSSIONS

In this study, to determine the response of two storeys building under blast effect, scaled distance parameter has been taking in consideration. After detonation, respectively for the scaled distance $Z = 0.32 \text{ [m/ (kg}^{1/3})]$ and $Z = 0.64 \text{ [m/ (kg}^{1/3})]$ results are obtained and these are used for comparison and evaluation of the retrofitted structure performance against explosion loads.

• Structure without retrofitting

As shown in Fig.5 a) and b), numerous cracks are produced on the structure, particularly on the lateral facade which is more exposed to the explosion where, the failure of some components of the masonry wall is observed. The damage is more considerable in the case of small scaled distance.

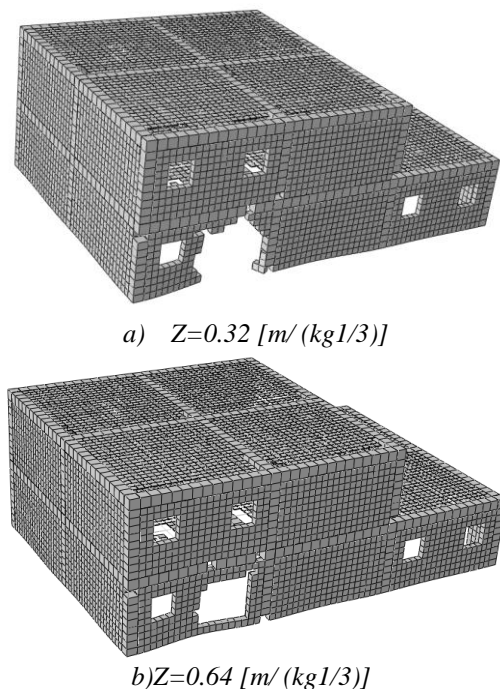


Figure 5. Structure without retrofitting under blast load.

• Strengthening structure with FRP

The performance of 2 mm thickness of FRP laminate on the lateral front face of the structure to strengthening the blast loading is studied. The mechanical properties of FRP for geometry are presented in Table 4. Numerical modeling results for strengthen facade against blast loading is illustrated in Fig. 6 a) and b). Results show in both cases of scale distances a reduction of cracks and non-failure of structural components.

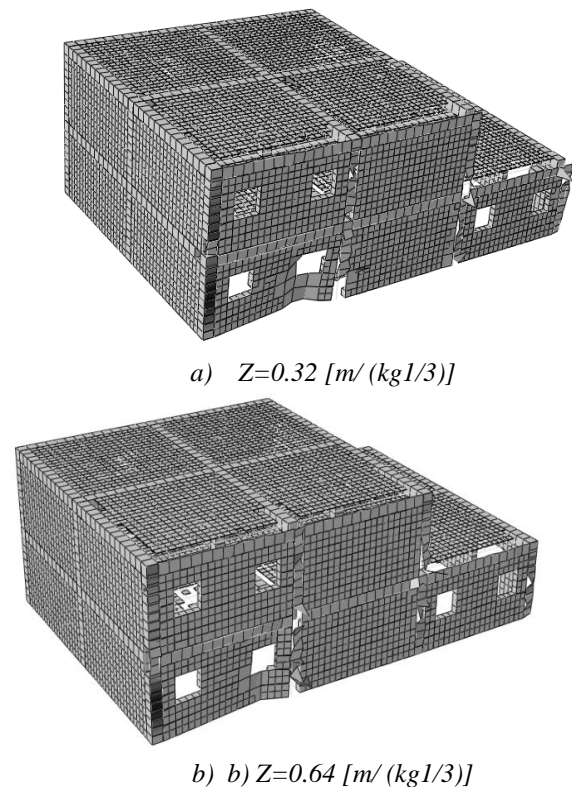


Figure 6. Strength structure performance with laminate FRP under blast load.

Strain energy of the building without retrofitting in both scaled distances is illustrated in Fig.7. For small value of scaled distance or low distance of blast position to structure increases the total energy, so that structure enters to the plastic area and causes its failure.

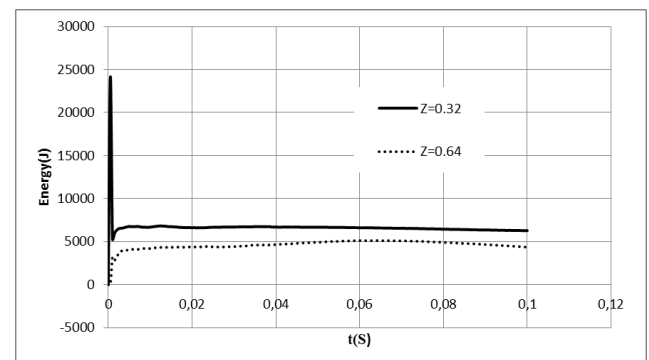


Figure 7. Strain Energy of the whole without retrofitting.

The strain energy of retrofitted facade with 2 mm lamina FRP in scaled distance $Z = 0.32 \text{ [m/ (kg}^{1/3})]$ is shown in Fig.8. Numerical simulation results demonstrated that the existence of FRP on the facade, by absorbing the strain energy, improves structure resistance to blast load.

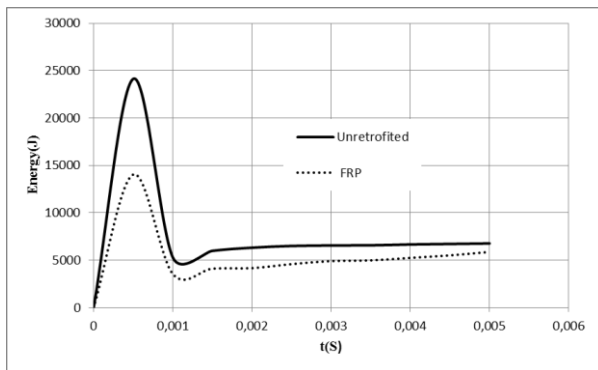


Figure 8. Strain Energy of the whole model $Z = 0.32$ [m/ (kg^{1/3})]

X. CONCLUSION

In this paper the nonlinear finite element method were developed to evaluate the behavior of two storeys building under blast load. Dynamic analysis was performed using ABAQUS software. Two stand-off distances have been used. According to the results of the simulated model, the strain energy increases when the scale distance becomes smaller. The effect on performance increasing, with the use of the FRP plates with optional thickness improves structure resistance against

REFERENCES

- [1] American Society of Civil Engineers (ASCE) (2011). "Blast Protection of Buildings." ASCE 59-18 11, Reston, Virginia.
- [2] Canadian Standards Association (CSA). (2012). "Design and Assessment of Buildings Subjected 32 to Blast Loads.", CSA S850-12, Mississauga, Ontario, Canada.
- [3] American Society of Civil Engineers (ASCE) (2011). "Blast Protection of Buildings." ASCE 59-18 11, Reston, Virginia.
- [4] Wang, W., Zhang, D., Lu, F., Wang, S.C., and Tang, F. (2012). "Experimental Study on Scaling 94 the Explosion Resistance of a One-Way Square Reinforced Concrete Slab Under a Close-95 in Blast Loading." International Journal of Impact Engineering, Vol. 49, 158-164.
- [5] Li, B., Nair, A., and Kai, Q. (2012). "Residual Axial Capacity of Reinforced Concrete Columns 67 with Simulated Blast Damage." Journal of Performance of Constructed Facilities, ASCE, 68 Vol. 26(3), 287-299.
- [6] Nassr, A.A., Razaqpur, A.G., Tait, M.J., Campidelli, M., and Foo, S. (2012). "Experimental 75 Performance of Steel Beams under Blast Loading." Journal of Performance of Constructed 76 Facilities, ASCE, Vol. 26(5), 600-619.
- [7] Stoddart, E.P., Byfield, M.P., and Tyas, A. (2014). "Blast Modeling of Steel Frames with Simple 88 Connections." Journal of Structural Engineering, ASCE, 140(1), CID: 04013027.
- [8] Rodriguez-Nikl, T., Lee, C., Hegemier, G.A., and Seible, F. (2012). "Experimental Performance 82 of Concrete Columns with Composite Jackets under Blast Loading." Journal of Structural 83 Engineering, ASCE, 138(1), 81-89.
- [9] Coughlin, A.M., Musselman, E.S., Schokker, A.J., and Linzell, D.G. (2010). "Behavior of 40 Portable Fiber Reinforced Concrete Vehicle Barriers Subject to Blasts from Contact 41 Charges." International Journal of Impact Engineering, 37 (5), 521-529.
- [10] Dennis, S.T., Baylot, J.T., and Woodson, S.C. (2002). "Response of 1/4-Scale Concrete Masonry 43 Unit (CMU) walls to blast." Journal of Engineering Mechanics, 128(2), 134-142.
- [11] Abou Zeid, B.M., El-Dakhakhni, W.W., Razaqpour, A.G., and Foo, S. (2011-a). "Response of 3 Arching Unreinforced Masonry Walls to Blast Loading." Journal of Structural 4 Engineering, ASCE, 137(10), 1205-1214.
- [12] Baylot, J.T., Bullock, B., Siawson, T.R., and Woodson, S.C. (2004). "Blast Response of Lightly 28 Attached Concrete Masonry Unit Walls." Journal of Structural Engineering, ASCE, 29 131(8), August 2005, 1186-1193.
- [13] Abou Zeid, B.M., El-Dakhakhni, W.W., Razaqpour, A.G., and Foo, S. (2011-b). "Performance 6 of Unreinforced Masonry Walls Rertofitted with Externally Anchored Steel Studs under 7 Blast Loading." Journal of Performance of constructed facilities, ASCE, 25(5), 441-453.
- [14] Al-Salloum, Y.A., and Almusallam, T. (2005). "Load Capacity of Concrete Masonry Block 10 Walls Strengthened with Epoxy-bonded GFRP Sheets." International Journal of Composite 11 Materials, 39 (19), 1719-1745.
- [15] Irshidat, M., Al-Ostaz, A., Cheng, A.H.D., and Mullen, C. (2011). "Nanoparticle Reinforced 55 Polymer for Blast Protection of Unreinforced Masonry Walls: Laboratory Blast Load 56 Simulation and Design Model." Journal of Structural Engineering, ASCE, 137(10), 1193-1204.
- [16] Mayrhofer, C. (2002). "Reinforced Masonry Walls Under Blast Loading." International Journal 73 of Mechanical Sciences, Vol. 44, 1067-1080.
- [17] Wu, C., Hao, H., and Lu, Y. (2005). "Dynamic Response and Dynamic Analysis of Masonry 100 Structures and Masonry Infilled RC Frames to Blast Ground Motion." Engineering 101 Structures, 27, 323-333.
- [18] Kinney, G.F., and Graham, K.J., Explosive Shocks in Air, 2nd Edition, Springer-Verlag, New York, 1985.
- [19] Ngo, T.; Mendis, P.; Gupta, A.; Ramsay, J. Blast Loading and Effects on Structures – An Overview EJSE Special Issue: Loading on Structures, 2007.
- [20] Technical Manual, Army TM5-1300, Navy NAVFAC P-397, Air Force AFR 88-22, Structures to resist the effects of accidental explosions, US Department of Commerce, National Technical Information Service, Washington, DC, 1990
- [21] Hopkinson, B. British Ordnance board minutes 13565, 1915
- [22] Cranz, C., Lehrbuch der Ballistik, Springer, Berlin, 1926
- [23] A.P. Mouritz, D.S. Saunders, S. Buckley, (1994). "The damage and failure of GRP laminates by underwater explosion shock loading", Composites 25 431-437.
- [24] ABAQUS/Explicit User's Manual, Version 6.1, V I & II, Hibbitt, Karlsson & Sorensen, Inc., 2000.
- [25] The Institute of Makers of Explosives (2014), TNT Calculator https://www.ime.org/content/tnt_calculator, Washington.